Linear to circular polarization conversion using microwave hybrids for VGOS (2-14 GHz)

O. García-Pérez, F. Tercero, I. Malo, J. A. López-Pérez

CDT Technical Report 2018-13

Observatorio de Yebes
Guadalajara (Spain)

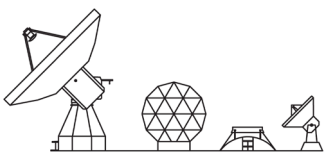

August, 2018

1 Introduction

VGOS (VLBI Global Observing Service, formerly VLBI2010) is the next generation of VLBI systems in which the traditional S/X stations are being replaced by modern wideband antennas covering the frequency range between 2 and 14 GHz with a single receiver [1]. For the implementation of the wideband feed antenna, most of the candidate designs are based on linearly polarized antennas, including Eleven [2], quasi self-complementary (QSC) [3], and quad-ridged flared horn (QRFH) [4] feeds. Few exceptions, such as the Dyson conical quad-spiral array (DYQSA) [5], are based on circularly polarized antennas, although in this case additional circuitry (i.e., wideband baluns and combiners) is required to get two single-ended output ports.

Radio astronomy observations, VLBI in particular, require receivers with dual circular polarization reception. Consequently, the use of linearly polarized feeds for VGOS could imply a conversion from linear to circular polarization at some point of the system. In particular, the following options may be considered: hardware at the front-end, or by digital reconstruction of the circular polarizations from linear ones [6]. This report deals with the first case, in which hybrid couplers are considered to directly convert the two linearly polarized signals from the feed into left- and right-handed circular polarizations (LHCP/RHCP). The axial ratio (or the corresponding cross-polar ratio) is used as figure of merit to evaluate the feasibility of this option.

2 Conversion from linear to circular polarization

In a general case, the electric field of a propagating electromagnetic wave traces out an ellipse in the plane normal to the direction of propagation. According to the notation used in Fig. 2.1, the polarization ellipse is characterized by its maximum and minimum field values (OA and OB), the sense of rotation, and the tilt angle (τ). The axial ratio (AR) is defined as

$$AR = \frac{\text{major axis}}{\text{minor axis}} = \frac{OA}{OB} = \frac{|E_{max}|}{|E_{min}|} \tag{2.1}$$

According to the previous definition, pure circular polarization corresponds to $|AR| = 1$, and in the case of linear polarization the axial ratio goes to infinite. These are the two extreme conditions, so any other case corresponds to elliptical polarization with certain axial ratio $1 \leq |AR| \leq \infty$.

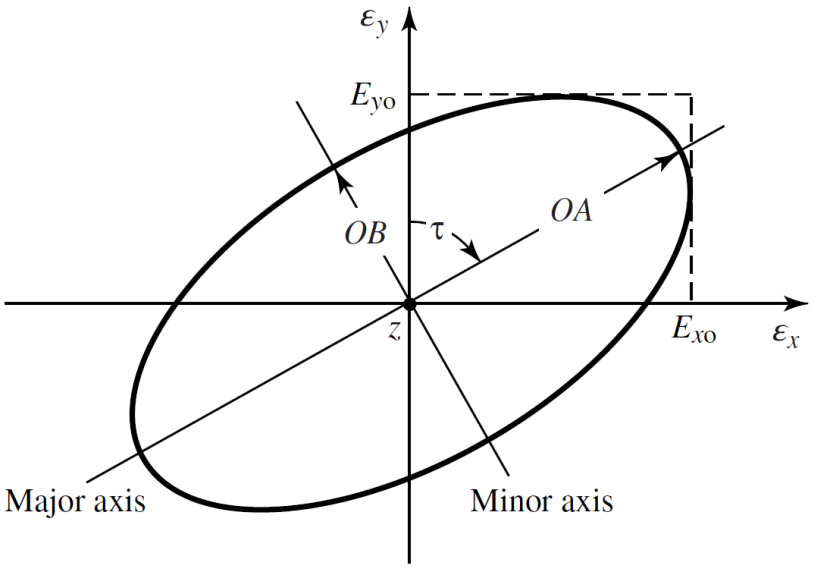

Fig. 2.1: Representation of the polarization ellipse.

The normalized electric field of a circularly polarized plane wave propagating along z-axis can be written as

$$\bar{E} = (\hat{x} \pm j\hat{y})/\sqrt{2} \tag{2.2}$$

where $\pm$ indicates the sense of rotation. According to (2.2), circular polarization can be obtained just by combining two equal and orthogonal linear excitations by adding $\pi/2$ phase difference between them. This can be directly implemented by using a 3dB/90-deg hybrid coupler.

Since actual couplers unavoidably show magnitude and phase unbalances, the obtained polarization will generally be nearly but not purely circular. Another practical issue that should be addressed is the use of a pair of cables between the antenna ports and the coupler input ports that are not identical. This translates into phase unbalances, which may be significant at higher frequencies.

Let's consider a wave propagating along z-axis formed by the combination of two x- and y-polarized waves

$$\overline{E_t} = E_{x0} \cdot e^{j\phi_x}\hat{x} \; + \; E_{y0} \cdot e^{j\phi_y}\,\hat{y} \tag{2.3}$$

where E_{x0} and E_{y0} are the amplitudes, and ϕ_x and ϕ_y are the phases of each individual field. The corresponding major and minor axes can be obtained as [7]

$$\begin{aligned} OA &= \sqrt{0.5\left(E_{x0}^2 + E_{y0}^2 + \sqrt{E_{x0}^4 + E_{y0}^4 + 2\cdot E_{x0}^2 E_{y0}^2 \cos\left(2\left(\phi_y - \phi_x\right)\right)}\right)} \\ OB &= \sqrt{0.5\left(E_{x0}^2 + E_{y0}^2 - \sqrt{E_{x0}^4 + E_{y0}^4 + 2\cdot E_{x0}^2 E_{y0}^2 \cos\left(2\left(\phi_y - \phi_x\right)\right)}\right)} \end{aligned} \tag{2.4}$$

which can be introduced in (2.1) to calculate the corresponding axial ratio.

At this point, it can be useful to analyze the particular case in which a real 90-deg coupler is used to excite an antenna with dual linear polarization, and to obtain the axial ratio in terms of the magnitude and phase errors introduced by the component. Following the notation introduced in (2.3), the errors in terms of amplitude (A) and phase ($\Delta\phi$) can be expressed as

$$\begin{aligned} A &= E_{x0}/E_{y0} \\ \Delta\phi &= \left(\phi_y - \phi_x\right) - \pi/2 \end{aligned} \tag{2.5}$$

so that the total electric field can be rewritten as

$$\overline{E_t} = \hat{x} \; + \; Ae^{j(\pi/2+\Delta\phi)}\,\hat{y} \tag{2.6}$$

It must be noted that the phase error $\Delta\phi$ is defined as the difference between the phase unbalance of the two output ports of the coupler and the ideal 90 deg that it should provide. In this case, the axial ratio in dB can be obtained as

$$AR_{\mathrm{dB}} = 10\cdot\log_{10}|AR|^2 = 10\cdot\log_{10}\left|\frac{1 + A^2 + \sqrt{1 + A^4 + 2\cdot A^2\cos\left(2\left(\frac{\pi}{2} + \Delta\phi\right)\right)}}{1 + A^2 - \sqrt{1 + A^4 + 2\cdot A^2\cos\left(2\left(\frac{\pi}{2} + \Delta\phi\right)\right)}}\right| \;(\mathrm{dB}) \tag{2.7}$$

A chart representing the axial ratio as a function of both amplitude and phase errors is shown in Fig. 2.2.

Alternatively, a simpler but approximated formula for the axial ratio is given in [8]

$$AR_{dB} \approx \sqrt{(A_{dB})^2 + 0.15^2 \cdot \left(\Delta\phi_{deg}\right)^2} \text{ (dB)} \tag{2.8}$$

where $A_{dB} = 10 \cdot \log_{10} A^2$, and $\Delta\phi_{deg}$ denotes the phase error in degrees. In some cases, this formula can be useful for rapid calculations by hand.

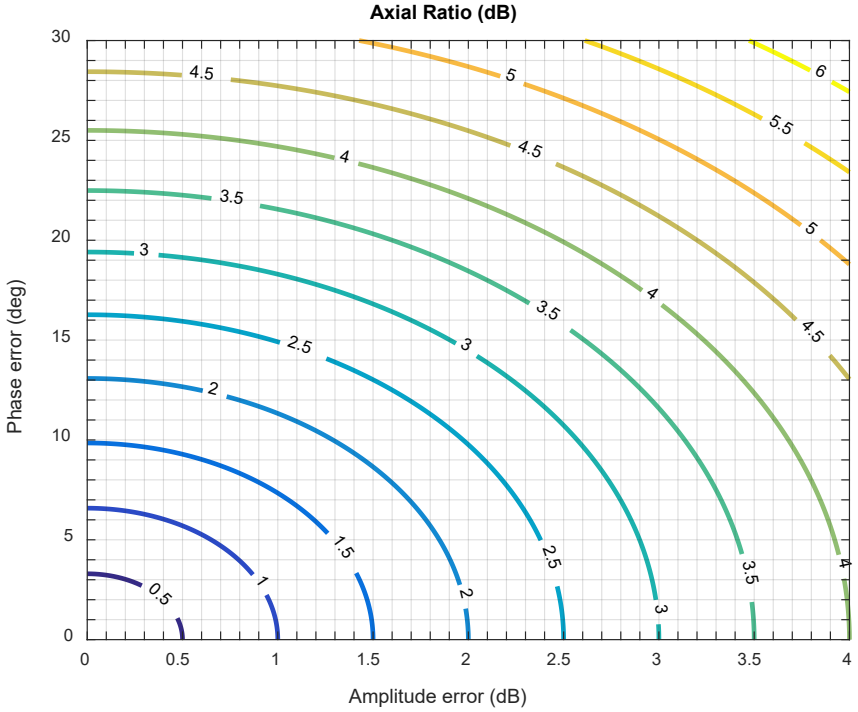

Fig. 2.2: Axial ratio as a function of amplitude and phase errors.

In addition, it is possible to define the polarization purity in terms of the cross-polar level as

$$XP_{dB} = 10 \cdot \log_{10}\left(\frac{|AR| - 1}{|AR| + 1}\right)^2 \text{ (dB)} \tag{2.9}$$

which denotes the discrimination between the circular co-polar and cross-polar components. The conversion chart between axial ratio and circular cross-polarization is represented in Fig. 2.3 [9].

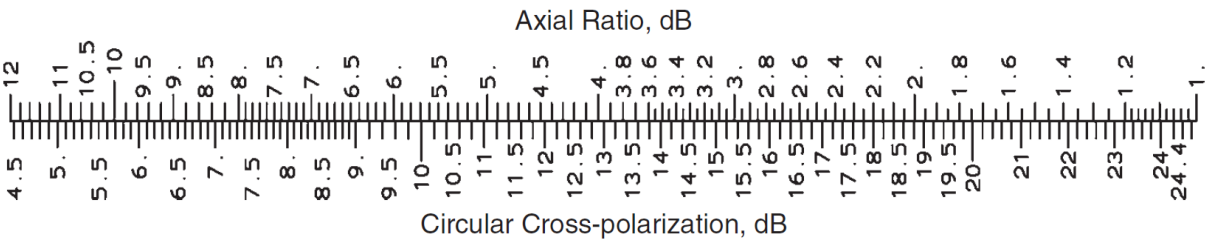

Fig. 2.3: Conversion chart between axial ratio and circular cross polarization.

3 Wideband hybrid couplers for VGOS

Multioctave stripline hybrids are proposed as potential candidates to achieve circular polarization for the frequency range of VGOS (i.e., 2-14 GHz) [10]. This type of coupler has been specifically designed to operate at cryogenic temperatures. The measured performance of one of these devices is presented in Fig. 3.1. Return loss is better than -20dB. The amplitude unbalance is lower than 0.9 dB, and the phase error is lower than 3 deg in the whole band.

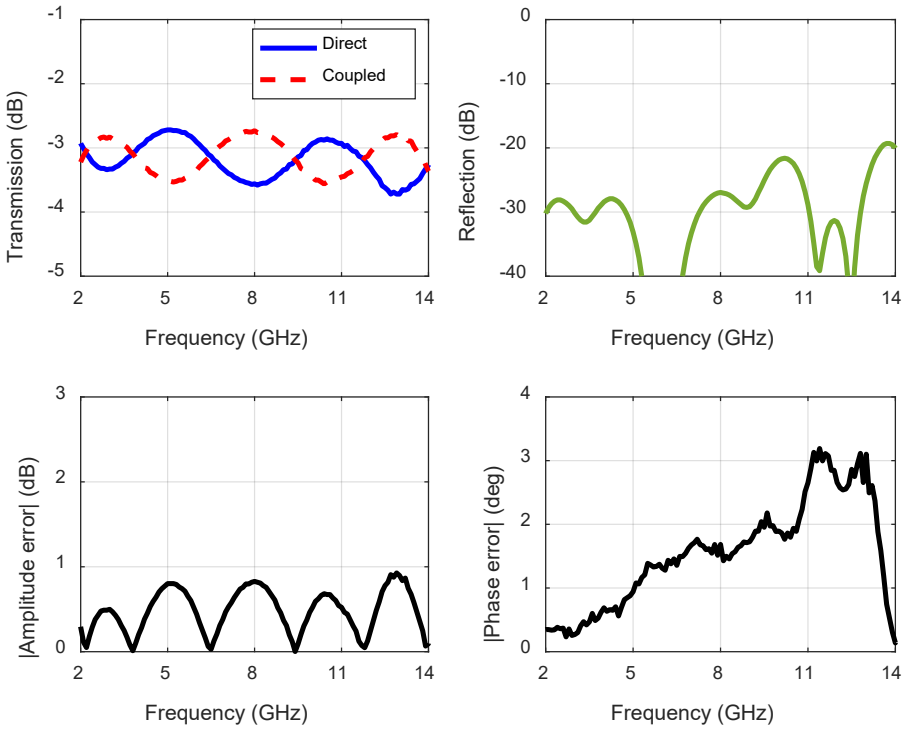

Fig. 3.1: Measured performance of the 90-deg hybrid coupler for VGOS.

4 Estimated performance

From the measured results of the hybrid, and based on the analysis presented in Section 2, it is possible to estimate the conversion to circular polarization that can be achieved with the coupler. For this purpose, the axial ratio has been evaluated using (2.7) and has been plotted in Fig. 4.1. Furthermore, the corresponding cross-polar discrimination is plotted in Fig. 4.2. As in the isolated coupler the amplitude error dominates over the phase error, the axial ratio is well approximated by the amplitude unbalance. Consequently, the axial ratio is lower than 1 dB throughout the entire frequency band. In terms of cross-polar discrimination, this corresponds to -25 dB for the worst case.

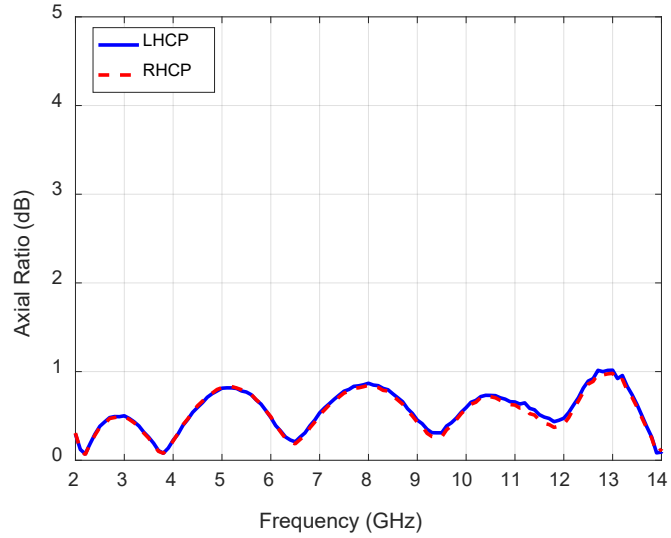

Fig. 4.1: Estimated axial ratio from the measured results of the coupler.

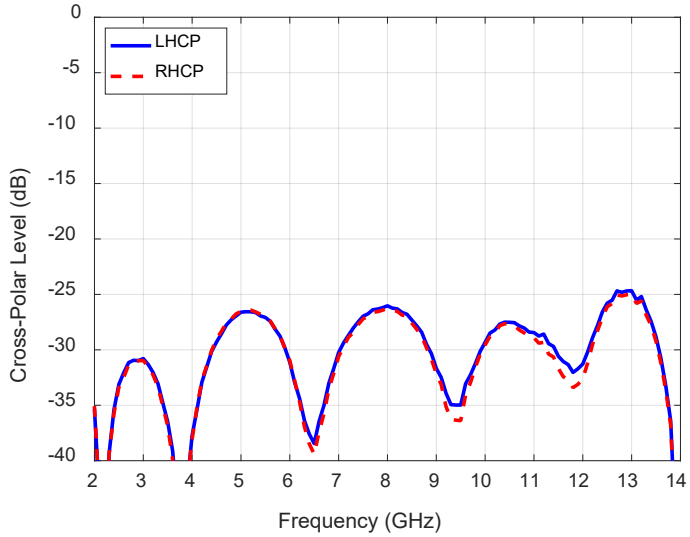

Fig. 4.2: Estimated cross-polar level from the measured results of the coupler.

As it was stated before, another important aspect that should be considered in a practical implementation is the phase difference introduced by the two connecting cables between the hybrid ports and the dual linearly polarized antenna ports. The phase constant of a PTFE coaxial cable is represented in Fig. 4.3. A difference in terms of length of 1 mm would correspond to phase difference of about 24 deg at 14 GHz. This term has direct effect on the axial ratio, since it is added as an extra term of the phase error. The axial ratio assuming differences of length between the connecting cables of 0.2, 0.5 and 1 mm is represented in Fig. 4.4, and the corresponding cross-polar discrimination is represented in Fig. 4.5. It can be observed how the effect of the cables is particularly noticeable at the higher part of the band.

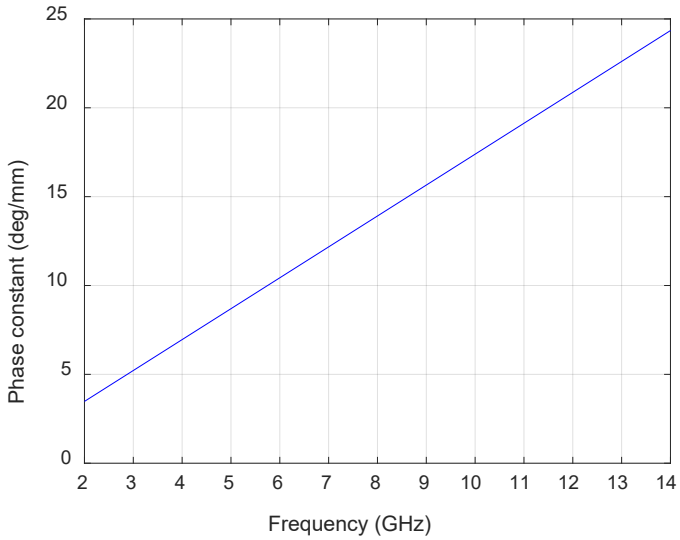

Fig. 4.3: Phase constant of a PTFE coaxial cable.

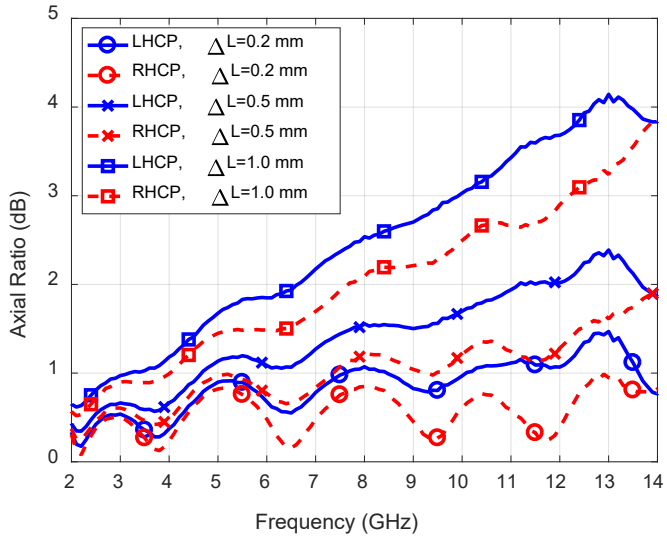

Fig. 4.4: Estimated axial ratio assuming differences in length ΔL between the connecting cables.

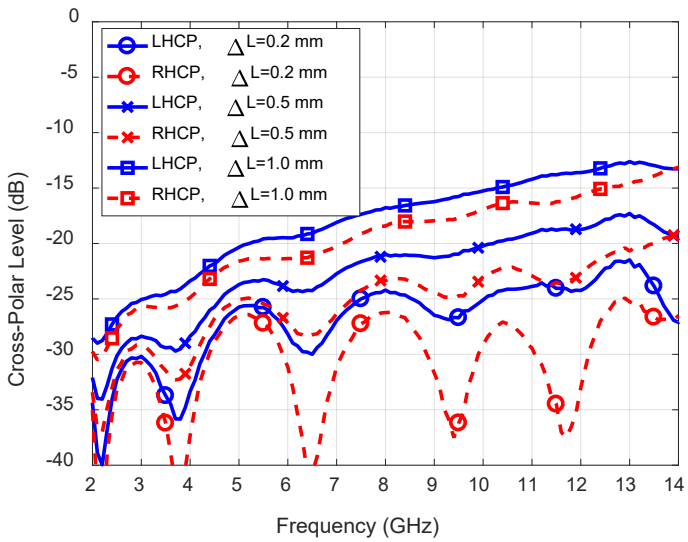

Fig. 4.5: Estimated cross-polar level assuming differences in length ΔL between the connecting cables.

5 Noise contribution

Finally, the noise contribution from this device to the receiver noise has been computed from actual measurements in Yebes laboratories. Fig. 5.1 shows the performance of a single-ended cryogenic LNA and a balanced LNA which uses this kind of 3dB/90deg hybrids. The difference in performance of these LNAs is a good estimation of the hybrid's noise contribution. It can be seen that the increment is 1-3 Kelvin in the range 2-14 GHz.

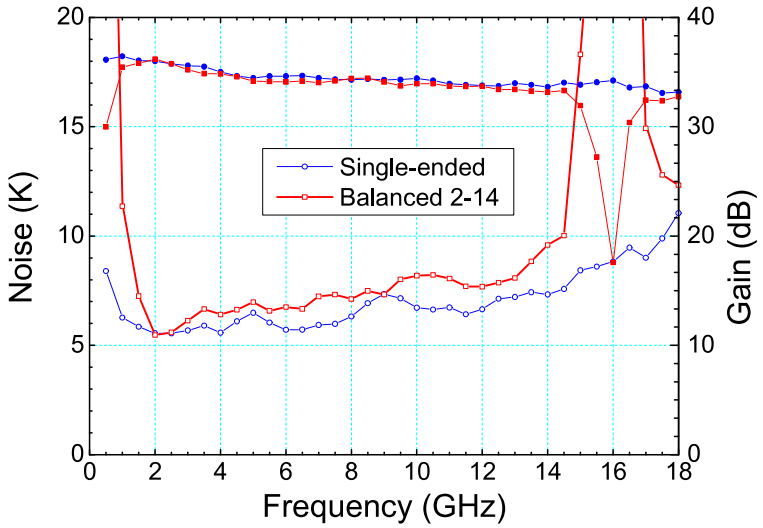

Fig. 5.1: Measured noise temperatures of cryogenic single-ended and balanced LNAs.

6 Conclusion

The use of wideband hybrid couplers to obtain circular polarization in a radio astronomy receiver using dual linear polarization antennas has been analyzed and evaluated. In particular, the frequency range of the VGOS project, i.e. 2-14 GHz, has been considered. Currently available couplers would allow typical values of axial ratio better than 1 dB. Nevertheless, such values are valid as far as the connecting cables are identical. It has been shown that length differences in the order of tenths of millimeter can introduce significant phase errors at high frequencies, which would degrade the overall axial ratio.

In addition, there is a little degradation in terms of noise performance (1-3 Kelvin). This degradation can be assumed if the benefits of having circular polarization using hardware are greater than using software.

Therefore, the ease and accuracy of software circular polarization recovery should be compared with this hardware option in order to select the best solution for VGOS.

References

[1] B. Petrachenko, "VLBI2010: Progress and Challenges," *IVS 2012 General Meeting Proceedings*, pp. 42-46, 2012.

[2] R. Olsson, P. Kildal, S. Weinreb, "The Eleven antenna: a compact low-profile decade bandwidth dual polarized feed for reflector antennas," *IEEE Trans. Antennas Propag.*, vol. 54, pp. 368-375, Feb. 2006.

[3] G. Cortes-Medellin, "Non-planar quasi-self-complementary ultra-wideband feed antenna," *IEEE Trans. Antennas Propag.*, vol. 59, pp. 1935-1944, Jun. 2011.

[4] A. Akgiray, S. Weinreb, W. Imbriale, et al., "Circular quadruple-ridged flared horn achieving near-constant beamwidth over multioctave bandwidth: design and measurementes," *IEEE Trans. Antennas Propag.*, vol. 61, pp. 1099-1107, Mar. 2013.

[5] E. Garcia, S. Llorente, A. Lampérez, et al., "Dyson Conical quad-spiral array as ultrawideband feed system," *Loughborough Antennas and Propagation Conference (LAPC)*, Nov. 2015.

[6] B. Petrachenko, "VLBI2010 digital processing requirements," *IVS Memorandum 2007-006v01*, Jul. 2007 [Online]. Available: http://ivscc.gsfc.nasa.gov/

[7] C. A. Balanis. *Antenna theory*. Wiley, 4th ed., 2016.

[8] S. V. Parekh, "Simple formulae for circular-polarization axial-ratio calculations," *IEEE Antennas Propag. Mag.*, vol. 33, pp. 30-32, Feb. 1991.

[9] T. A. Milligan. *Modern antenna design*. Wiley. 2nd ed., 2005.

[10] I. Malo-Gómez, J. D. Gallego-Puyol, C. Díez-González, et al., "Cryogenic hybrid coupler for ultra-low-noise radio astronomy balanced amplifiers," *IEEE Trans. Microw. Theory Tech.*, vol. 57, pp. 3239-3245, Nov. 2009.